ELSEVIER

Journal of Membrane Science 5224 (2002) 1–9

journal of MEMBRANE SCIENCE

www.elsevier.com/locate/memsci

Effect of cell configurations on the performance of citric acid production by a bipolar membrane electrodialysis

Xu Tongwen*, Yang Weihua

Department of Applied Chemistry, University of Science and Technology of China, Hefei 230026, China

Received 21 June 2001; accepted 19 November 2001

Abstract

The purpose of this study was to evaluate the effect of cell configurations on the energy consumption and the electroacidification parameters in the production of citric acid using a bipolar membrane electrodialysis (BPED). Three basic cell arrangements, A (anion membrane)–C (cation membrane)–BP (bipolar membrane)–A–C (type I), C–BP–C (type II) and BP–A–C–BP (type III) were discussed and compared. Type I generates acid citrate by acidification with acid sulfate produced from the dissociation of sodium sulfate, and type II produces acid citrate by replacing Na^+ with H^+ generated at BPED and type III generates acid citrate by direct splitting sodium citrate. The current density–voltage curves for the three configurations show the typical behaviors given by the coupling of ion transport and electrical field-enhanced water dissociation and are not completely overlapped in the two determined orders due to the change in Donnan potential at the bipolar junction and solution–membrane interface. The magnitudes of cell voltage, current efficiency and energy consumption follow the analogous order as type II < type I < type III, while the potential drop across a bipolar membrane follows the order type II > type I ≈ type III. From the comprehensive considerations of the energy consumption, current efficiency and concentration of the produced acid citrate, it suggests that type II seems to be a favorable cell configuration for the production of citric acid. It is not advisable to manufacture acid citrate by direct splitting its salt. © 2002 Published by Elsevier Science B.V.

Keywords: Bipolar membrane; Citric acid; Cell configuration; Water dissociation

1. Introduction

Conventionally, most organic acids are produced from fermentation process followed by precipitation and chemical acidification. The product obtained by this technique is usually at low concentration, e.g. 0.2–1N due to the limitation of fermentation process. Because the fermentation process typically operates at near neutral pH; this being maintained via addition of a suitable base. Increasing the product concentration significantly reduces the productivity of the fermentor due to product inhibition. One more disadvantages of this method include denaturation of some organic/amino acid on exposure to alkali and acid treatment, high ash content and large discarding of wastes produced from the filtration and precipitation processes.

Bipolar membrane water splitting technology provides an attractive complement to the fermentation technology by removing the product acid, while simultaneously providing an equivalent amount of base for use in adjusting the pH in the fermentor. The fermentor itself can now be operated at relatively low product concentration to assure high productivity. As an added advantage the produced acid is usually at a relatively high concentration so that the subsequent purification via crystallization or other techniques is rel-

* Corresponding author. Tel.: +86-551-360-1587.
E-mail address: twxu@ustc.edu.cn (X. Tongwen).

0376-7388/02/$ – see front matter © 2002 Published by Elsevier Science B.V.
PII: S0376-7388(01)00795-5

atively inexpensive. This technology has been used in several industries/investigated in experimental set-ups for producing organic/amino acids [1–4] such as lactic acid [5], citric acid [6], acetate acid [7] as well as electroacidification of soybean protein [8–10].

The principle of the electrodialytic water-dissociation process employing a bipolar membrane (BP) is well documented. If a direct electrical potential (dc) is established between a bipolar membrane which consists of a layer of an anion exchange membrane and a layer of a cation exchange membrane, water dissociation occurs at the interphase and a current is sustained through the membrane by the migration of hydrogen and hydroxyl ions to the respective compartments under the fluency of applied dc electric field. By appropriately arranging conventional cation-exchange and anion-exchange membrane on either side of the bipolar membrane, cations and anions of a given organic salt, e.g. sodium citrate (Na_3Cit) as discussed here, could be so directed to meet the OH^- and H^+ in respective compartments to generated separate streams of alkali and citric acid (H_3Cit). This new technology is not only related with the operation conditions but at large extent, related to the configurations of bipolar membrane cell stacks as well [4,11,12].

Therefore, the main purpose of current research is to investigate the effect of the cell configurations on H_3Cit production based on water dissociation with bipolar membranes. We try to correlate the results of the current density–voltage (*I–V*) curve, current efficiency and energy consumption with the cell configurations.

2. Experimental

The laboratory-scale experimental set-up was composed of one anode and one cathode as well as different number of cation-, anion- and bipolar exchange membranes inserted between them, forming three different cell configurations as described below.

2.1. A–C–BP–A–C type (type I)

This arrangement is shown in Fig. 1 (a) and consists of a bipolar membrane (BP) operating in conjunction with two cation exchange membranes (C) and two anion exchange membranes (A). This is a standard six-compartment stack in conjunction with the electrodes. The 0.5 M sodium citrate solution is fed to the acid chamber between the cation side of the bipolar membrane and the anion membrane and 0.5 M sodium sulfate solution fed to the other chambers if not specifically mentioned. This configuration generates acid citrate in the chamber between the cation side of bipolar membrane and anion membrane by acidification with acid sulfate produced from the dissociation of sodium sulfate.

2.2. C–BP–C type (type II)

This arrangement is shown in Fig. 1 (b) and consists of a bipolar membrane (BP) operating in conjunction with two cation exchange membranes (C) to form a four-compartment stack in combination with the cathode and anode. The 0.5 M sodium citrate solution is fed to the acid chamber between the cation side of the bipolar membrane and the cation membrane neighboring to the cathode and 0.5 M sulfate sodium solution fed to the other chambers if not specifically mentioned. The organic salt is converted into organic acid with the protons produced from the water dissociation transporting into the chamber and the sodium ions out of the chamber. In this case, acid citrate is formed by replacing Na^+ with H^+ in the chamber between the cation side of bipolar membrane and cation membrane.

2.3. BP–A–C–BP type (type III)

This arrangement is shown in Fig. 1 (c) and consists of two bipolar membranes (BP) operating in conjunction with an anion exchange membrane and a cation exchange membrane (C) to form an analogous five-compartment stack in combination with the cathode and anode. The 0.5 M sodium citrate solution is fed to the chamber between the anion and cation exchange membranes and 0.5 M sodium sulfate fed to the other compartments if not specifically mentioned. This type generates acid citrate by direct splitting sodium citrate in the chamber between the cation side of the bipolar membrane and the anion membrane.

Both the ion exchange membranes and bipolar membranes used here are prepared from our lab. The cation exchange membrane was prepared by sulphonating poly(phenylene oxide) (PPO) [13], the

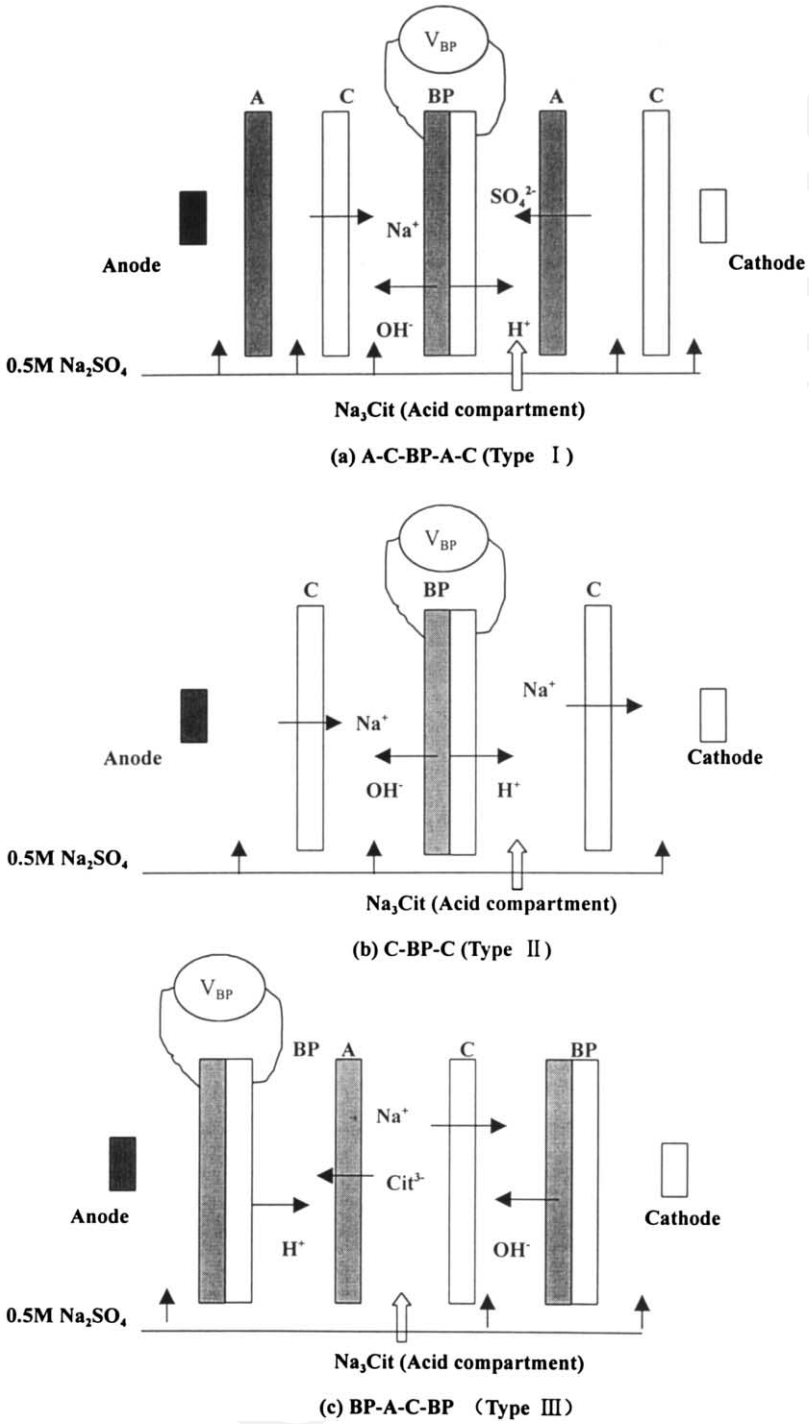

Fig. 1. Scheme of the laboratory cell configurations for citric acid production by electrolytic dialysis (ED) with bipolar membranes.

Table 1
Characteristics of the electrodialytic stack and the membranes

Number of the cell triplets	1
Cationic membrane	Interpolymer type, sulfonic group
Area resistance ($\Omega\,cm^2$)	1.6–2.0
Anionic membrane	Interpolymer type, quarternary ammonium group
Area resistance ($\Omega\,cm^2$)	2.4–3.0
Bipolar membrane	Composition of the cationic and anionic membranes
Area resistance ($\Omega\,cm^2$)	5.0–8.0
Effective membrane area (cm^2)	20
Cell thickness (cm)	0.2
Electrodes	Expanded titanium metal net coated with precious metal oxide
Effective volume of solution circulated in each compartment (ml)	500
Flow arrangement	Parallel

anion exchange membrane is prepared by brominating and quarter-aminating PPO [14] and the bipolar membrane is obtained by casting the cation layer solution onto the anion layer [15]. The salient features of the stack and the membranes are given in Table 1.

The dc potential was established between the end electrodes of the stack through a CV/CC regulated power supply (YJ63, Shanghai Huguang Instruments works). The voltage drop across the stack was directly read from the indicators on the power supply, while the potential drop across a bipolar membrane was measured with a Digital multimeter (model:GDM-8145, Good will instrument Co. Ltd., Taiwan) through two platinum probes near to the two surfaces of the layers. After the electrodialytic stack was assembled, the streams were circulated at a flow rate of 2.5 l/h from different reservoirs. At a given time, the solution in acid compartment was sampled and the concentration of citric acid was determined by titration with standard sodium hydroxide solution using phenolphthalein as indicator.

The experiments were of batch-type operation. Each data point was averaged from three independent experimental runs.

3. Results and discussions

3.1. Current–voltage curves

The current–voltage curves were measured under the condition of 0.5 M sodium citrate in acid chamber and 0.5 M Na_2SO_4 in the other chambers for the three cell configurations except that for type I the curves was also measured under symmetrical concentration of 0.5 M Na_2SO_4. It should be noted that all the curves were determined in the two orders: one is from the low current densities to high densities (upwards) and the other is from the high densities to low densities (downwards). The results are depicted in Figs. 2 and 3. Obviously, the experimental *I–V* curves for the three configurations show the typical behavior given by the coupling of ion transport and electrical field-enhanced water dissociation [16,17]: at small voltage, the current is carried mainly by the salt ions and attains a limiting value. The resistance of the membrane is more or less increased due to the migration of salt ions out of the bipolar junction; at high voltage, most of the current is carried by the H^+ and OH^- ions generated by water dissociation tak-

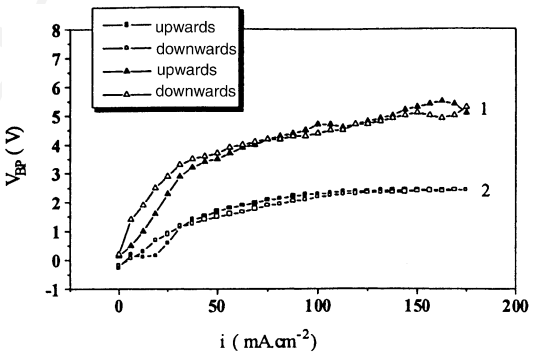

Fig. 2. Experimental *I–V* curves for A–C–BP–A–C unit: (1) solutions in all compartments are 0.5 M Na_2SO_4 solution; (2) solution in acid compartment is replaced by 0.5 M citric sodium.

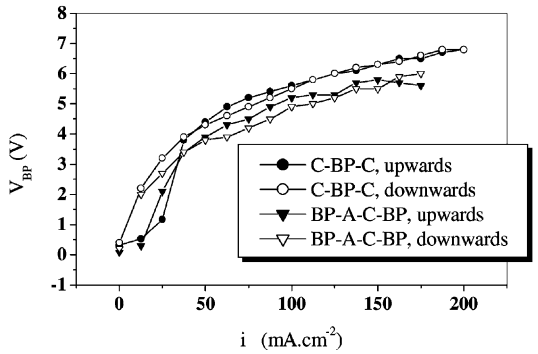

Fig. 3. Experimental *I–V* curves for C–BP–C–BP cell units: 0.5 M citric sodium in acid compartment and 0.5 M Na_2SO_4 in the other ones.

ing place at the bipolar junction, and increases rapidly with the voltage. The membrane resistance then begins to decrease again with the applied voltage. However, the magnitudes of voltage values across bipolar membrane in the considered current density range for type I in the different electrolyte are significantly different. The voltages measured under symmetrical concentration of 0.5 M Na_2SO_4 are appreciably larger than those obtained in the case of sodium citrate contained in the acid chamber (Fig. 2). This is mainly due to two reasons: one reason is that the conductivity of 0.5 M sodium sulfate solution (2.82×10^4 μS/cm, determined by DDS 11A conductivity meter, Shanghai Leici, China) is higher than that of 0.5 M sodium citrate solution (2.13×10^4 μS/cm); another one is that part of strong electrolyte sodium citrate is transfer to weak electrolyte acid citrate due to water dissociation during the *I–V* measurements. The relative magnitude of voltages at the case of sodium citrate for different configurations is not clearly observed and will be discussed in the follow at a current density $I = 100\,\text{mA/cm}^2$. In addition, *I–V* curves in the two orders are not completely overlapped, especially at the case of low current densities. This result may be explained considering the structures of the bipolar membrane and ionic composition changes in the two orders. As mentioned above, the bipolar membrane used in this paper is prepared by casting cation membrane solution onto an anion membrane and with an asymmetrical layer thickness. This membrane structure will easily cause a change in Donnan potential at the bipolar junction and solution-membrane interface when the ionic composition is changed by water dissociation at upwards direction before downwards measurements are conducted and thus caused a change in whole potential drop across a bipolar membrane [18]. Nevertheless, the Donnan potential is less compared with the applied voltage at high current density [19], that is why the deviation is less obvious at high current densities than that at the low ones.

3.2. Voltage across the cell stack at a typical current density

Cell voltage is an important parameter because it is related to energy consumption associated with the production of an acid and a base based on bipolar membranes. The voltage drop, which refers to the variation that take place in the ED cell, mainly includes the Donnan potential at all solution–membrane interface and diffusional potential both in the mono-exchange membrane and in the solution as well as the voltage across a bipolar membrane. So, it is connected with the number of the compartments and the concentration of solution in the compartments and thus related with cell configurations. Values of the voltage drop for the three types of cell arrangement at a typical current density $I = 100\,\text{mA/cm}^2$ are plotted in Fig. 4. It can be noticed that when a constant current was applied (galvanostatic conditions), the cell voltage drops keep approximately constant, indicating that the water dissociation at this condition approaches to be steady state. When the cell voltages are compared within different cell arrangements, it is interesting to find the values increase in the order: type II < type I < type

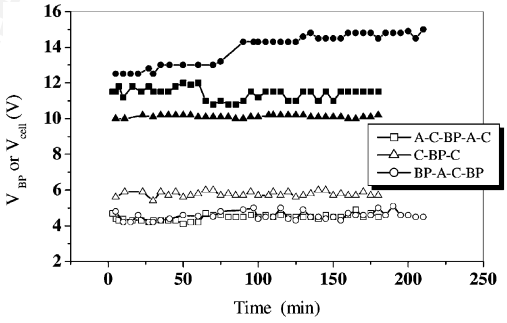

Fig. 4. Time dependence of the voltages across the cell (solid symbols) and BP (open symbols) at $I = 100\,\text{mA/cm}^2$ for different cell configurations.

III. A difference of the order of ∼4.5 V was observed among the three type of cell configurations. It is not difficult to understand the voltage order type II < type I because type I has the equal number of bipolar membrane as the type II but two more mono-membranes and chambers as shown in Fig. 1. It is well known that the voltage across a bipolar membrane has a relatively large contribution to the cell voltage at the state of water dissociation [16,17]. Thus the cell voltage in type III has the largest value among the considered configurations because it contains one more bipolar membrane. When the potentials across the bipolar membrane for different configurations are compared, the values follow the order: type II > type I ≈ type III. This is possibly due to the concentration change in the adjacent chambers of the bipolar membrane. For type I, the electrolyte concentration at both adjacent chambers of BP increases due to the production of H^- and OH^- and the migration of Na^+ and $SO_4{}^{2-}$ from the other chambers. For type III, the situation is analogous. But for type II, the electrolyte concentration in the chamber between cation side of bipolar membrane and the cation membrane will not increase with the dissociation process, moreover, part of sodium citrate is transformed into weaker electrolyte citric acid ($pK_1 = 3.13$). This is why the voltage across the bipolar membrane for type II is higher than the other two cases. However, this deviation is not so large as the difference of cell voltage.

3.3. Current efficiency

The current efficiency η was calculated as [7]

$$\eta = \frac{(C_0 - C_t)VF}{NIt} \quad (1)$$

where C_0 and C_t are the equivalent concentration of citric acid (acid compartment) at time 0 and t, respectively. V is the circulated volume of solution in each compartment, I the current, F the Faraday constant and N the number of cell triplets.

The current efficiency is determined by various time intervals from the beginning and therefore it is dependent of time. As shown in Fig. 5, the current efficiency decreases with time which conforms to the typical trends, thereby restricting the possibility of obtaining high concentration of acid and alkali [7]. As can be seen from Fig. 5, at a given time, the magnitude of current efficiencies for the three cell configurations follows the order: type III < type II < type I. Theoretical interpretation to this order can be based on the ionic transport and molecular diffusion in different cell arrangements.

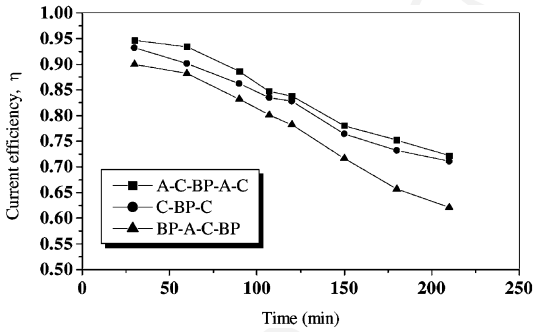

Fig. 5. Current efficiencies for citric acid production vs. time at $I = 100\,mA/cm^2$.

As shown in Fig. 1(a), when a direct current is passed between the electrodes in type I cell stack, protons produced from cation side of bipolar membrane are introduced into the acid compartment and acidify the organic salt into the corresponding acid at the same time. In this process neither other cations compete with H^+ nor anions with sulfate. So the current efficiency is relatively high. For type II, the citric is formed in a manner analogous to the above by a direct current. In this arrangement, of course, there are some possibilities that the produced H^+ ions competitively electro-transport and citric acid diffuses through the cation membrane to the neighboring compartment to that of the acid chamber. However, in this experimental conditions, the other cations such as Na^+ (0.5 M Na_2SO_4 + 0.5 M Na_3Cit = 2.5 N Na^+) have a very high concentration compared with the H^+ and at the same time, the cation membrane has a strong repulsion to the coions, Cit^{3-} ions. Therefore, both the competitive transport of H^+ ions and the diffusion of citric acid seem to be not significant. The large possibility that decreases the current efficiency will be caused by the neutralization of acid with base transported through cation membrane from the cathode compartment under the electrical field, because cation membrane is not completely selective to hydroxyl ions. In addition, the concentration of citric acid also tend to be decreased by the water transport from the cathode com-

partment to the acid compartment due to the thinner of mono-cation membrane and the slight difference of the hydrodynamic conditions in these two compartments. This is supported by the volume change of solution in the acid and cathode compartments during the experiments. So the current efficiency in this type is a little lower than that in Type I.

In type III, acid citrate is formed by H^+ from BP and citrate transported from anion membrane as shown in Fig. 1(c). In addition that the unfavorable factors as mentioned above decrease the current efficiency, there exists a large possibility of competitive diffusion of OH^- ions with citrate, which came from the following hydrolysis reactions.

$$Cit^{3-} + H_2O \Leftrightarrow HCit^{2-} + OH^-$$

$$HCit^{2-} + H_2O \Leftrightarrow H_2Cit^- + OH^-$$

This competitive diffusion will considerably decrease both the current efficiency and acid concentration. On the other hand, citrate is larger compared with sulfate, its diffusion speed through the membrane will be lower than sodium or sulfate, which is also responsible for the decreased current efficiency. This configuration thus tends to achieve a relatively low acid concentration, which has been supported by the trends in the acid concentration in relation with increasing time as presented in Fig. 6.

It should be pointed out that citric acid is a weak electrolyte experiencing a considerably reduced Donnan exclusion to an anion or cation exchange membrane, there exists a possibility to be lost by diffusion into the neighboring compartment through an anion or cation membrane in all the three types [7]. This diffused acid also decreases the current efficiency so that the experimental current efficiencies are within 95% as shown in Fig. 5.

3.4. Energy consumption

The energy consumption E (kWh/kg) was calculated by extrapolating the results for the production of 1 kg of citric acid based on Eq. (2) [7]

$$E = \int \frac{UIdt}{(C_t VM)} \quad (2)$$

Here, U is the potential across the cell stack (V), M is the molar weight of citric acid (192 g/mol). The results, shown in Fig. 7, indicate that the energy consumption follows the order: type II < type I < type III which completely conforms to that of cell voltage. However, the difference of the energy consumption between the types is not proportional to that of cell voltage because the energy consumption is determined not only by the cell voltage but also by the amount of produced organic acid as shown in Eq. (2). Fig. 7 also shows that the energy difference between different cell configurations increases with an increase in the current density.

Therefore, both the current efficiency and the energy consumption are significantly affected by the cell configurations. In this study, we find that type III has the highest energy consumption but lowest current efficiency, it suggests that manufacture of organic acid is not advisable from the direct dissociation of its salts. Elecoacidification (type I) or ionic replacement (type

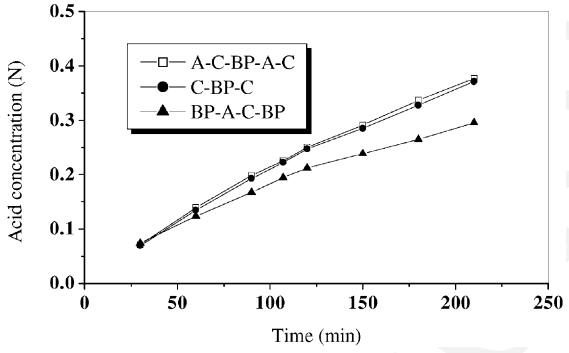

Fig. 6. Time dependence of citric acid concentration in the acid compartment ($I = 100\,mA/cm^2$).

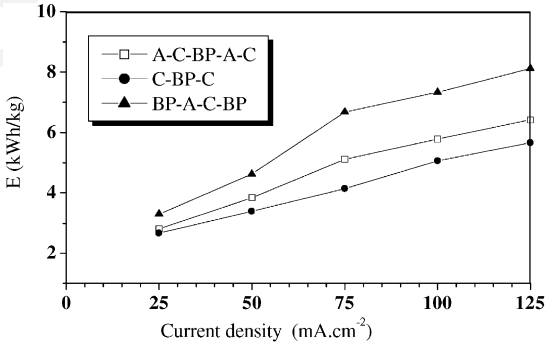

Fig. 7. Energy consumption for the production of citric acid production vs. current density.

II) with BPED is feasible, especially, type II is recommended due to its relatively low energy consumption and simplicity in unit construction though its current efficiency is a little less than that of type II. Nevertheless, better energy consumption values can be obtained by means of a filter type press ED cell in which the compartment thickness and the hydrodynamic conditions are more favorable in order to obtain better current efficiencies at the same time.

It should be noted that calculation of energy consumption is based on the total voltage drop across the stack. It might be lower in the practical use when there are many cell units. The reason is that the voltage drop in the anode and cathode chambers can be neglected when the cell units are many while if there is only one cell unit, the voltage drop across the anode and cathode chamber will cover a little ratio of the total voltage. However, it will not affect the relative magnitude of the investigated configurations because the anode and cathode compartments are same for these configurations.

4. Conclusions

Electrodialysis with bipolar membranes (BPED) provides a convenient way to produce citric acid. In this kind of operation, cell configurations plays an important role on the BPED characteristics.

The current density–voltage curves were measured under the asymmetrical concentration of 0.5 M sodium citrate in the acid chamber and 0.5 M Na_2SO_4 in the others based on two orders and three fundamental cell arrangements. The curves for the three configurations show the typical behavior given by the coupling of ion transport and electrical field-enhanced water dissociation and are not completely overlapped in the two determined orders due to the change in Donnan potential at the bipolar junction and solution–membrane interface.

The cell voltages, BP potential drop, current efficiency and energy consumption are discussed with the configurations of the cell stacks. The magnitudes of cell voltage follow the order: type II < type I < type III and the potential drop across a bipolar membrane the order: type II > type I ≈ type III. The current efficiency follow the order type II > type I > type III and energy consumption follow the order type I < type II < type III. From the comprehensive considerations of the energy consumption, current efficiency and concentration of the produced acid citrate, it suggests that type II seems to be a favorable cell configuration for the production of citric acid. It is not advisable to manufacture acid citrate by direct splitting its salt.

It should be mentioned that the above results are obtained with just one production cell between electrode compartments. For a commercial BPED stack with many production cells, the exact values for voltage drop, energy consumption and current efficiency may be changed due to the cell number. However, the relative magnitude of the investigated configurations is expected to be unchanged as long as the basic unit remains the same, because those parameters are seriously affected by ionic transport and molecular diffusion, which are independent of the interior cell number. So, the preliminary results can be act as a basis to investigate a commercial BPED stack with many units for a real citrate fermentation broth, which is scheduled in our lab and will be reported later.

Acknowledgements

Financial supports from Natural Science Foundation of Anhui Province (99045431), the Natural Science Foundation of China (No. 29976040, 20106015), Key Foundation of Educational Committee of Anhui Province (2000jl255zd), and the Foundation of Resources and Environments of University of Science and Technology of China are gratefully acknowledged.

References

[1] L. Bazinet, F. Lamarche, D. Ippersiel, Bipolar-membrane electrodialysis: applications of electrodialysis in the food industry, Trends Food Sci. Tech. 9 (1998) 107.
[2] H. Grib, L. Bonnal, R. Sandeaux, et al., Extraction of amphoteric amino acids by an electromembrane process-pH and electrical state control by electrodialysis with bipolar membranes, J. Chem. Technol. Biotechnol. 73 (1998) 64.
[3] A.L. Quoc, F. Lamarche, J. Makhlouf, Acceleration of pH variation in cloudy apple juice using electrodialysis with bipolar membranes, J. Agr. Food Chem. 48 (2000) 2160.

[4] T.W. Xu, Development of bipolar membrane-based processes, Desalination 140 (2001) 247.
[5] E.G. Lee, S.H. Moon, Y. K Chang, et al., Lactic acid recovery using two-stage electrodialysis and its modeling, J. Membr. Sci. 145 (1998) 53.
[6] S. Novalic, K.D. Kulbe, Separation and concentration of citric acid by means of electrodialytic bipolar membrane technology, Food Technol. Biotech. 36 (1998) 193.
[7] G.S. Trivedi, B.G. Shah, S.K. Adhikary, V.K. Indusekhar, R. Rangarajan, Studies on bipolar membranes. Part II.Conversion of sodium acetate to acetic and sodium hydroxide, Reactive Funct. Polym. 32 (1997) 32.
[8] L. Bazinet, F. Lamarche, D. Ippersiel, Comparison of chemical and bipolar-membrane electrochemical acidification for precipitation of soybean proteins, J. Agr. Food Chem. 46 (1998) 2013.
[9] L. Bazinet, F. Lamarche, D. Ippersiel, Effect of number of bipolar membranes and temperature on the performance of bipolar membrane electroacidification, J. Agr. Food Chem. 45 (1997) 3788.
[10] L. Bazinet, F. Lamarche, D. Ippersiel, Bipolar membrane electroacidification to produce bovine milk casein isolate, J. Agr. Food Chem. 47 (1999) 5291.
[11] T.W. Xu, W.H. Yang, B.L. He, Water dissociation phenomena in a bipolar membrane—the configurations and theoretical voltage analysis, Sci. China 42 (1999) 589.
[12] T.W. Xu, W.H. Yang, B.L. He, The functions and configurations of a bipolar type ion exchange membrane electrolytic cell (in Chinese), Chinese J. Membr. Sci. Technol. 20 (2000) 53.
[13] T.W. Xu, W.H. Yang, B.L. He, Ionic conductivity threshold in SPPO matrices: a combination of three-phase model and percolation theory, Chem. Eng. Sci. 56 (2001) 5343.
[14] T.W. Xu, W.H. Yang, Fundamental studies of a new series of anion exchange membranes: membrane preparation and characterisation, J. Membr. Sci. 190 (2001) 159.
[15] T.W. Xu, B.L. He, Z.M. Liu, Preparation and characterization of a new kind of bipolar membrane, in: Proceedings of the Annual Conference on Polymers, Vol. 2, Hefei, China, 1997, c47–48.
[16] H. Strathmann, J.J. Krol, H.J. Rapp, G. Eigenberger, Limiting current density and water dissociation in bipolar membranes, J. Membr. Sci. 125 (1997) 123.
[17] T.W. Xu, W.H. Yang, B.L. He, A simple model to determine the trends of electric field enhanced water dissociation in a bipolar membrane, Chinese J. Chem. Eng. 9 (2001) 179.
[18] T.J. Chou, A. Tanioka, Membrane potential of composite bipolar membrane in ethanol–water solutions: the role of the membrane interface, J. Colloid Interf. Sci. 212 (1999) 293.
[19] T. Aritomi, T. Boomgaard, H. Strathmann, Current–voltage curve of a bipolar membrane at high current density, Desalination 104 (1996) 13.